

# 3D DENSITY SCANS OF A SUPERSONIC GAS JET FOR BEAM PROFILE MONITOR

H. Zhang<sup>#</sup>, V. Tzoganis, K. Widmann, C. Welsch

Cockcroft Institute and The University of Liverpool, Warrington, WA44AD, UK

## Abstract

Recently, we have developed a novel beam profile monitor based on a supersonic gas jet. It can be applied to some extreme situation while other methods are not applicable such as for the high intensity and energy beams with destructive power and for the short life beam which requires minimum interference. The resolution of this monitor depends on the jet thickness and homogeneity, and thus we developed a movable gauge to investigate the gas jet distribution in a 3D manner. In this paper, we will present the measurement of the distribution of the gas jet and discuss the future improvement for the jet design.

## INTRODUCTION

Beam profile monitors are essential diagnostics for particle accelerators. With undergoing constructions of proposed high intensity and high power machine like ESS or HL-LHC, the conventional invasive diagnostics are not well suited because of the destructive beam power. Previously, IPM and BIF were used in similar situations based on the ionization or excitation of residual gas by the projectile beams [1]. The usage of the residual gas makes the diagnostic non-invasive but the signal level is low requiring long integration. Recently, a supersonic gas jet based monitor [2-4] was developed at the Cockcroft Institute. Using the gas jet with a high directional speed

and high density, the probability of ionization or excitation of the gas molecules will increase dramatically. Therefore, the integration time will be much reduced, even to a level where shot to shot measurement will be possible.

Previously, we reported the results of such monitor to measure a two-dimensional profile of a 5 keV, 7uA electron beam. [4]. Preliminary results have shown that the jet properties could affect the monitor performance. However, the jet homogeneity and density distribution is still unknown.

In this paper, we will present a subsystem dedicated to measure the gas jet profile in 3D and results about the jet density and homogeneity will be discussed in details.

## GAS JET SETUP AND MEASUREMENT

The details of the setup are shown in figure 1 and were described previously [4-6]. The supersonics gas jet is generated by injecting high pressure gas (1-10 bar) from gas tank pass through a small nozzle with diameter 30 μm into a low pressure region (10<sup>-4</sup> mbar). With further collimations, the gas jet can travel mono-directionally and be shaped into a screen-like curtain for diagnostic purpose. The differential pumping sections were designed to remove collimated gas molecular and maintain an ultra-high vacuum environment in the interaction chamber. Dumping sections are used for dumping the jet.

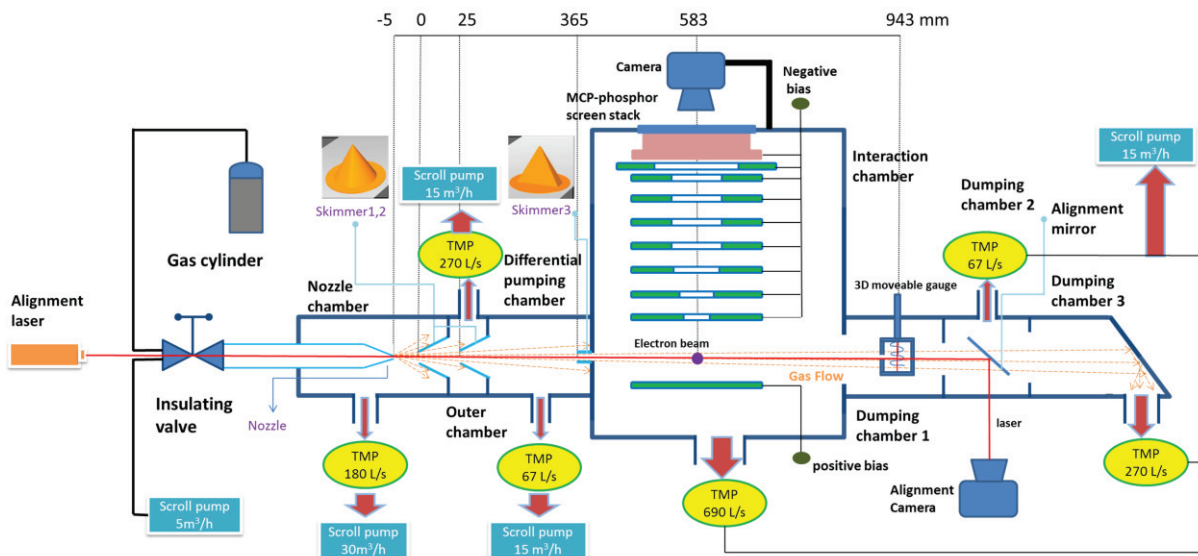


Figure 1: Schematic drawing of the complete setup.

#hao.zhang@cockcroft.ac.uk

The beam image of a 5 keV and 10  $\mu$ A electron beam was detected by collecting the ions using external electric field and MCP-phosphor screen stack, where the ions are generated by the interaction of the E-beam and the gas jet and represent the distribution of the projectile E-beam. One representative measurement is shown in figure 2.

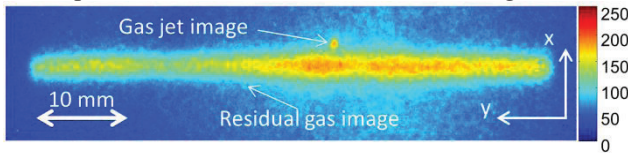


Figure 2: Images of the electron beam from both gas jet and residual gas.

### 3D MOVEABLE GAUGE SYSTEM

To measure the density distribution of the supersonic gas jet, a compression gauge solution [7] is adapted here. Based on that principle, we have installed a 3D moveable ion gauge assembly [8]. The assembly includes a CF Full Nipple DN40CF as shown in figure 3 with the bottom side closed by a fixed flange and the other side attached to a Granville Phillips Series 274 Nude Gauges. This component is then connected with a VACGEN MiniMax XYZ manipulator powered by three stepper-motors to allow a 3-dimensional movement with a resolution of 5  $\mu$ m. On the tube of the nipple 40 mm above the bottom, there is a 10 mm (length) \* 0.5 mm (width) slit which is the only opening to accept the gas flow.

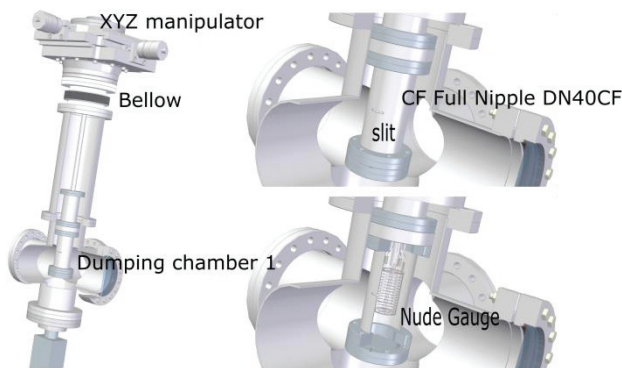


Figure 3: Mechanic drawing of the movable gauge system.

The gauge is powered by a VG IGC26 ion gauge controller and its signal is amplified by a pico-ampere meter and then recorded by oscilloscope. After the jet is fired, part of the jet enters the tube, the gas molecules accumulate inside and the density is measured by the gauge. If we assume that the gas diffusion is a much faster process than when gas molecular enters the tube, it will distribute equally immediately, the net gross rate of gas molecular inside the tube will be proportional to the gradient of the signal strength. Note that the baseline signal represents the stagnation density of the gas molecules inside the tube. Since the ion gauge itself is a heat source, and the heat inside the tube is not easy to be dissipated, continuous operation of the gauge will cause

the baseline signal to increase and possibly overflow the pico-ampere meter. To prevent that, special care were taken regarding the timing of the whole system by using the emission inhibit function of the gauge controller. The full timing table is shown in Figure 4. Note when the gauge inhibit is low the ion gauge is switched on and initially there will be a sudden rise of signal for the gauge reading due to the initialization. Therefore, there is a long delay between the gauge switched on and the pulse valve open to allow the gauge signal to return to the normal baseline.

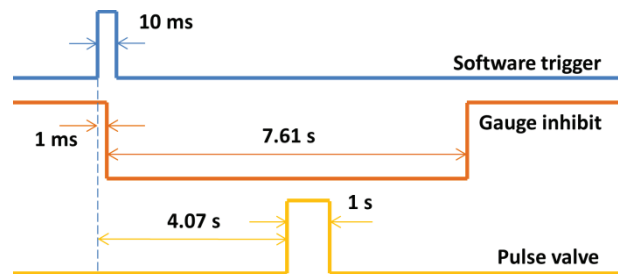


Figure 4: Timing diagram.

Typical measurements are shown in figure 5, where two processes can be identified. A quicker rise of the signal closely following the pulse valve trigger indicates the jet entering the tube while the slow rise indicates the density gradient flow from the background gas.

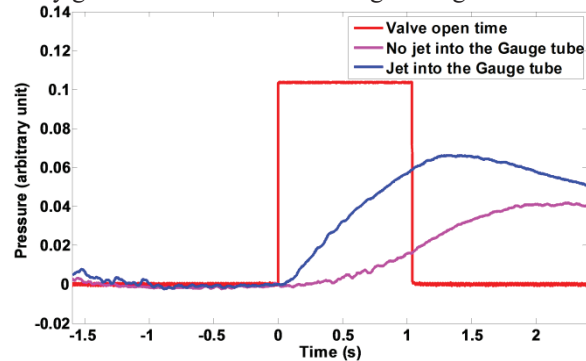


Figure 5: Pressure measured at the movable ionisation gauge.

With the software trigger generated by a control PC, the whole 3D scanning can be easily automated as the flow chart shown in figure 6.

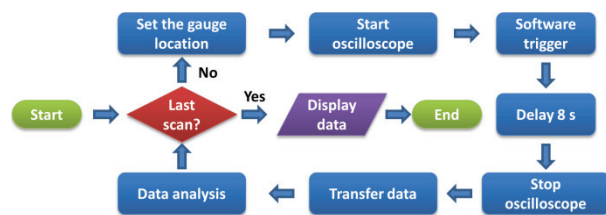


Figure 6: Data collection and analysis flow chart.

As shown in Figure 5, during the pulse valve gate time, the gradient of the gauge signal represent the number of gas molecular change. We choose the linear growth part of the signal, e.g. from 0.24 s to 0.56 s after the pulse

valve open, which will be better to reflect the change due to the gas jet. Then we fit the data to find the gradient which will represent the number density change inside the tube. We did four transverse 2D scans with different longitudinal position from -1.5 mm to 0 mm of the jet with a transverse range of 12.5 mm \* 20 mm with a step size of 0.5 mm. The data is shown in Figure 7. For all cases, the horizontal size is about 10.0 mm and the vertical size is about 5.5 mm. The difference among them is quite small and it could be due to the fact that we don't have enough transverse resolution or the growth of the jet size is small to be detected in a 1.5 mm range.

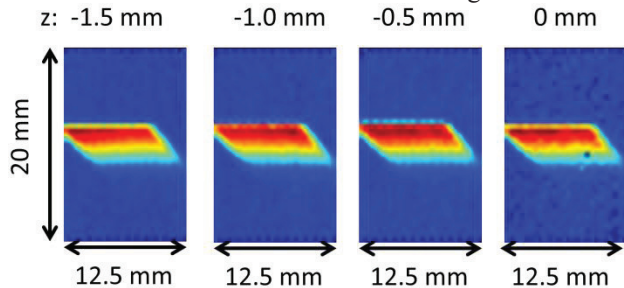


Figure 7: Normalized number density change recorded by a moveable gauge with a rectangular slit.

In the horizontal axis, since the length of the slit is much larger than the jet waist, the number density change will be a constant in the middle of the slit and only drops when the jet is intercepted by the edge of the slit. Thus, the distribution measured here will be dominated by the slit length no matter how small the step size is. However, if we differentiate the value of the number density change around the edges in its horizontal axis, we can obtain the normalized density distribution along the horizontal axis. The smaller the step size is the finer distribution we get after differentiation. Vertically, because the slit width is much smaller than the jet length and comparable to the step size, we can use the measured distribution in the vertical axis as the jet density distribution directly.

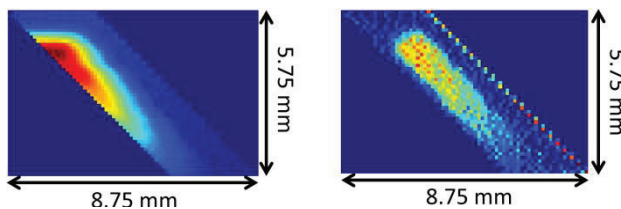


Figure 8: Edge scan and the associated jet density distribution.

Based on this, we did a finer scan with a step size of 0.125 mm only around the left edge of the previous scan as shown in the left image of Figure 8. By differentiating the result in horizontal axis, we get a normalized jet density distribution image as shown in the right side of Figure 8. The size of the jet is measured as 5.44 mm \* 1.55 mm in full width, and the tilted angle is 42.9 degree. With originally 4.0 mm \* 0.4 mm, the length of the jet increased 1.36 times and the width of the jet increased 3.88 times which indicate the growth is non-isotropic.

From the measurement of the normalized jet distribution, we can estimate the jet size in the interaction location assuming a linear expansion in each direction, which is 4.66 mm \* 0.92 mm. Then the jet thickness contribution to the uncertainty of the measurement  $\sigma_{jet}$  will be [4]

$$\sigma_{jet} = \frac{w_{jet}}{2\sqrt{3}\cos(\theta)}$$

where  $w_{jet}$  is the width of the jet 0.92 mm and  $\theta$  is the Jet angle 42.9 degree, which gives  $\sigma_{jet}$  as 0.36 mm. Previous analysis reported a lower value of  $\sigma_{jet}$  because we assumed the jet would keep its aspect ratio.

## CONCLUSIONS

In this paper, we describe a system to measure the 3D density distribution of a supersonic jet used as a beam profile monitor. Details are presented about the mechanical setup and relevant components, timing system and measurement procedure as well as the measurement results. Current measurements about the transverse profile of the jet further corrects the model we use to estimate the uncertainty from the jet width when measure y size of the projectile beam. Further work can be done to calibrate this system to get the absolute value of the 3D jet density under different operation condition such as stagnation gas pressure from the gas tank, different skimmer sizes and locations and different gas species. Comparison with simulation data is undergoing which will allow us to optimize the monitor system to produce better jet suitable for measuring the projectile beam profile more efficiently and accurately.

## ACKNOWLEDGMENT

This work is supported by the Helmholtz Association under contract VH-NG-328, the European Union's Seventh Framework Programme for research, technological development and demonstration under grant agreement no 215080 and the STFC Cockcroft core grant No. ST/G008248/1.

## REFERENCES

- [1] P. Forck, *Proceedings of IPAC2010*, Kyoto, Japan, pp. TUZMH01, 2010.
- [2] V. Tzoganis and C. P. Welsch, *Appl. Phys. Lett.*, vol. 104, no. 20, 2014.
- [3] H. Zhang, *et al.*, *Proceedings of IPAC2016*, Busan, Korea, pp. MOPMR046, 2016.
- [4] H. Zhang, *et al.*, submitted to *PRAB*.
- [5] V. Tzoganis, *et al.*, *Vacuum*, vol. 109, pp. 417–424, 2014.
- [6] M. Putignano, PhD thesis, University of Liverpool, 2012.
- [7] Y. Hashimoto, *Proceedings of IBIC2013*, Oxford, UK, pp. WEPF17, 2013.
- [8] H. Zhang, *et al.*, *Proceedings of IBIC2015*, Melbourne, Australia, pp. TUPB075, 2015.